Green Chemistry

PAPER

View Article Online
View Journal | View Issue

Cite this: *Green Chem.*, 2016, **18**, 1715

High efficiency single-step biomaterial-based microparticle fabrication *via* template-directed supramolecular coordination chemistry†

Kwok Kei Lai,[a] Reinhard Renneberg[a] and Wing Cheung Mak*[b,c]

Biomaterial-based microparticles have attracted much attention for medical and biological applications such as pharmaceutics, bioseparation and cosmetics. Emerging technologies enable versatile and facile fabrication of microparticles, with key features being purity, precise size control, mild preparation conditions and minimal processing. Here, an innovative approach combining template synthesis, biomolecule assembly and partial-purification within a single step for high efficiency fabrication of pure biomaterial-based microparticles is reported. This concept is based on facile co-precipitation of biomolecules within $CaCO_3$ templates and simultaneous crosslinking of entrapped biomolecules *via* Ca^{2+} driven supramolecular coordination chemistry, followed by template removal. Carbohydrate (alginate) and proteins (casein and fresh milk) are used as models of biomolecules. The process driven by selective crosslinking automatically excludes non-specific materials from the template and thus provides the additional function of partial-purification, as demonstrated using highly complexed fresh milk. This green approach to fabrication of biomaterial-based microparticles offers three critical advantages (i) mild conditions to preserve the chemical and secondary structures of biomolecules; (ii) single processing step to facilitate scale-up production; and (iii) partial-purification without the need for upstream raw material purification. This innovative approach not only addresses fundamental issues in fabrication techniques, but also marks progress in energy and environmental conservation during manufacturing processes.

Received 8th October 2015,
Accepted 3rd November 2015

DOI: 10.1039/c5gc02424b

www.rsc.org/greenchem

1. Introduction

Microparticles and nanoparticles composed of biomaterials have garnered research attention in recent decades due to their existing and expected utility in medical applications,[1] biosensing,[2] food industry,[3] *etc*. Their small size offers a high surface-area-to-volume ratio for surface modifications, rapid absorption and rapid digestion. Current applications under investigation include but are not limited to cellular imaging,[4] drug delivery,[5] high throughput bead-based bioassay,[6] regenerative medicine,[7] food packaging,[8] *etc*. In addition, sensitive or fragile small molecules can potentially be loaded inside the core of biomaterial-based microparticles, thus gaining protection against harsh environments. Accordingly, micro and nano-particles have also been extensively studied as carriers for vaccines.[9,10] In these various applications, the ultimate goal is often to improve human health and standards of living. Therefore, all components constituting the final microparticle must be biocompatible and safe for daily human administration. This requirement can be fulfilled by using natural sources of biomaterials as building blocks for biocompatible microparticles and nanoparticles. Peptides and carbohydrates are two main categories of natural biopolymers that are abundantly available from both animal and plant sources. They are generally biocompatible and edible, as are most proteins and sugars. Existing methods for producing biomaterial-based microparticles include multiple emulsion systems (W/O, W/O/W, *etc*.),[11] spray drying,[12] photolithography,[13] coacervation,[14] layer-by-layer assembly,[15] *etc*. Recently, $CaCO_3$ have been widely used as a facile and biocompatible scaffold for producing microparticles. Among different crystalline $CaCO_3$ morphologies, porous $CaCO_3$ such as vaterite[16] is capable of loading various molecules that can potentially be used in drug delivery and biosensing applications.[17,18] After loading with desired molecules, the $CaCO_3$ scaffold was substantially coated by multiple layers of polyelectrolytes using the Layer-by-Layer

[a]*Department of Chemistry, Hong Kong University of Science and Technology, Clear Water Bay, Hong Kong, P. R. China*
[b]*Department of Physics, Chemistry and Biology, Biosensors and Bioelectronics Centre, Linköping University, 58183 Linköping, Sweden*
[c]*Integrative Regenerative Medicine Centre, Department of Clinical and Experimental Medicine, Linköping University, SE 58185 Linköping, Sweden. E-mail: wing.cheung.mak@liu.se*

†Electronic supplementary information (ESI) available. See DOI: 10.1039/c5gc02424b

(LbL) technique[19,20] or by additional chemical crosslinking processes and washing steps[21] for microparticle formation. Finally, the $CaCO_3$ template was removed by ethylenediaminetetraacetic acid (EDTA). However, these methods are tedious and time consuming, and usually require synthetic crosslinkers that may reduce compatibility and viability.[22–24] Research groups have previously reported the fabrication of organic–inorganic hybrid micro-structures by mixing $CuSO_4$ and proteins without the use of crosslinkers.[25,26] The reported fabrication processes, though less laborious, require a considerable amount of time (at least 24 h).

With these considerations in mind, we present in this paper a highly efficient single-step green approach for producing biomaterial-based microparticles by a $CaCO_3$ templating technique. This smart approach hinges on the dual function of Ca^{2+}, as a component for formation of the $CaCO_3$ template and a crosslinker for entrapped biomolecules *via* supramolecular coordination chemistry. In other words, entrapment of biomolecules and crosslinking is completed simultaneously in a single step in the scale of seconds, without the need for additional synthetic crosslink reagents and incubation steps. Moreover, the proposed $CaCO_3$ templating technique allows for precise control over size of microparticles as demonstrated in our previous work.[27] The $CaCO_3$ template can be easily removed by a mild acidic environment, leaving behind vacant internal space/pores from the sacrificial template for post-loading of desired drugs or nutraceuticals. The technique is applicable to different drugs by selection of appropriate microparticle building blocks to enhance loading efficiency. For example, hydrophobic drugs may be loaded by using β-casein as the building block as it is composed of highly hydrophobic peptide sequences.

This fabrication concept is demonstrated using both casein and alginate as protein and carbohydrate models, respectively. Casein is a well characterized protein present in milk, which has several subtypes including α_s, β, κ, γ, *etc*. Among them, β-casein is Ca^{2+} sensitive and binds with Ca^{2+} ions, forming a stable assembly.[28] On the other hand, alginate is extensively used in encapsulation, as building blocks of biocompatible 3D structures, *etc*.[29] When Ca^{2+} is added, the alginate molecules in the solution stack together according to the 'egg-box' model, forming a stable hydro gel.[30] In nature, Ca^{2+} and other metal ions serve as important coordination crosslinkers in providing structural and mechanical strength in organisms.[31,32] This is crucial for normal growth and cellular functions for plant and animal cells.[33–35]

In both models, we have proven Ca^{2+} coordination chemistry driven microparticle formation. The morphologies and surface zeta potential, as well as chemical and secondary structure of the biomaterial-based microparticles, were characterized. We have further demonstrated that this protocol is capable of preparing purified microparticles using a highly complex biomaterial mixture (fresh milk). The composition of the product is elucidated by sodium dodecyl sulfate polyacrylamide gel electrophoresis (SDS-PAGE) and Fourier transform infrared (FTIR) analysis.

Overall, the proposed fabrication procedure involves only naturally available materials, with all reactions taking place under ambient conditions, eliminating the need for extreme temperature and pressure.[36,37] Also, organic solvents and synthetic crosslinkers are not required throughout the process. With minimal input of extra energy, harmful ingredients and pollution output, this fabrication process presents itself as a green protocol for the production of microparticles for biomedical applications.

2. Experimental

2.1. Materials

Casein sodium salt from bovine milk (Grade III) and alginic acid sodium salt from brown algae (viscosity of 2% solution at 25 °C approximately equals 3500 cps) were purchased from Sigma (St. Louis, MO, USA). Calcium chloride (minimum 96%, powder, anhydrous), sodium carbonate (minimum 99.8%, anhydrous, ACS reagent) and hydrochloric acid (37%, ACS reagent) were purchased from Sigma-Aldrich (St. Louis, MO, USA). An Amplite™ Colorimetric Calcium Quantitation Kit was purchased from AAT Bioquest® Inc. (Sunnyvale, CA, USA). Sodium dodecyl sulfate (minimum 90%) was purchased from Riedelde Haën (Seelze, Germany). Precision Plus Protein™ Unstained Standards, 10× Tris/Glycine/SDS running buffer, 40% Acrylamide/Bis Solution (37.5 : 1), *N*,*N*,*N*′,*N*′-tetramethylethylenediamine (TEMED), 1.5 M Tris-HCl buffer pH 8.8, Coomassie Brilliant Blue R-250 staining solution and Coomassie Brilliant Blue R-250 Destaining solution were purchased from Bio-Rad Laboratories, Inc. (Hercules, CA, USA). Ammonium persulfate (minimum 98%, ACS reagent) was purchased from USB® Molecular Biology Reagents and Biochemicals (Cleveland, Ohio, USA). Fresh milk (calcium content = 1.1 mg mL^{-1}; fat content = 35 mg mL^{-1}) was purchased from the local supermarket. All chemicals were being used directly after purchase without further purification.

2.2. Fabrication of biomaterial-based microparticles

Casein and milk microparticles used throughout this work were prepared as follows. Casein (20 mg mL^{-1}) in d.d. H_2O (250 μL) or fresh milk (without pre-treatment) was rapidly mixed with $CaCl_2$ (1 M) in d.d. H_2O (250 μL) and Na_2CO_3 (0.5 M) in d.d. H_2O (500 μL) under magnetic stirring in a beaker for 30 s. The reaction mixture containing casein or milk loaded $CaCO_3$ templates was collected and washed by centrifugation with d.d. H_2O 5 times to remove excess raw materials. Finally the templates were removed by acid titration using HCl (6 M) to pH 5. The microparticles yielded were immediately washed by centrifugation with d.d. H_2O 3 times, then resuspended in d.d. H_2O and kept at 4 °C for later experiments.

Alginate microparticles used throughout this study were prepared as follows. Alginic acid (5 mg mL^{-1}) in d.d. H_2O (250 μL) was first mixed with Na_2CO_3 (0.5 M) in d.d. H_2O (500 μL). This solution was then added dropwise to a beaker containing $CaCl_2$ (1 M) in d.d. H_2O (250 μL) under vigorous magnetic

stirring. The reaction mixture containing alginate loaded $CaCO_3$ templates was collected and washed by centrifugation with d.d. H_2O 5 times to remove excess raw materials. Finally the templates were removed by acid titration using HCl (6 M) to pH 5. The microparticles yielded were washed by centrifugation with d.d. H_2O 3 times, then resuspended in d.d. H_2O and kept at 4 °C for later experiments.

2.3. Scanning electron microscopy (SEM)

The surface morphology of the protein microparticles was characterized by scanning electron microscopy. Before examination, the microparticles were washed by centrifugation with d.d. H_2O 3 times. They were then dropped onto silicon wafers which were affixed on copper stages by using a carbon adhesive tape and silver paint (Structure Probe, Inc., West Chester, PA, USA). After drying the particle samples in a desiccator (humidity <40%), the whole stage was coated by a single layer of gold using a sputter coater K575X (Quorum Emitech, UK). The SEM images were recorded with JSM-6700F or JSM-7100F (JEOL, Japan) at 5 kV.

2.4. Particle size and zeta potential measurement

The particle size and zeta potential of microparticles were measured by using a ZetaPlus zeta-potential analyzer (Brookhaven Instrument Corporation, USA). About 1.5 mL of microparticles suspended in d.d. H_2O were loaded into a cuvette for each measurement. The number of runs per measurement equalled 5. In addition, image analysis software ImageJ (NIH, USA) was employed for measuring particle size on SEM images.

2.5. SDS-PAGE

Composition analysis of casein and milk-based microparticles was carried out by means of SDS-PAGE. Casein microparticles, milk microparticles, fresh milk (diluted to 0.125×) and casein (1 mg mL^{-1}) were separately incubated with 5× SDS sample buffer in a ratio of 4 : 1 in 95 °C heat block for 10 min. After that, 8 μL from each sample and 10 μL molecular weight ladder were first loaded into wells of 5% stacking gel which were then separated by 15% resolving polyacrylamide gel. A constant voltage of 150 mV was applied to the gel tank (Mini-PROTEAN® 3 Cell, Bio-Rad, CA, USA) for 1.5 h until the leading dye had almost reached the bottom of the polyacrylamide gel. The gel was then rinsed by d.d. H_2O and stained by Coomassie Brilliant Blue for 30 min in an orbital shaker. The staining solution was subsequently discarded and replaced with Coomassie Destaining solution for removing the background color. Finally, the polyacrylamide gels were placed onto a desktop scanner (Perfection 610, Epson) to record the protein bands.

2.6. Colorimetric quantification of Ca^{2+} concentration

The amount of Ca^{2+} within the microparticles was quantified by using an Amplite™ Colorimetric Calcium Quantitation Kit, which has a dye that changes its color when bound to Ca^{2+}. The analysis was carried out in a 96-well microtiter plate according to the assay protocol given in the kit. In brief, a standard calcium ion concentration calibration curve was established from 0 μM to 150 μM. Then, the microparticle suspensions (50 μL) were mixed with the supplied dye (50 μL) in the well and incubated in the dark for 10 min for color development. The color change after the reaction was measured by using a FluoStar Optima spectrophotometer (BMG LABTECH, Ortenberg, Germany) at 600 nm. For control experiments, alginate solution, casein solution and fresh milk with the same concentration as their corresponding microparticle suspension were prepared accordingly. 50 μL from each sample were mixed with 50 μL of dye and the color changes were quantified by the same protocol as mentioned above.

2.7. FTIR

FTIR spectra were obtained using a VERTEX 70 (Bruker, USA) equipped with a germanium attenuated total reflectance (ATR) sample cell. Microparticle suspensions and their corresponding raw material solutions were dropped onto the surface of the ATR cell and FTIR spectra were recorded in the frequency region of 400–4000 cm^{-1} with a resolution of 4 cm^{-1} for 16 cycles.

3. Results and discussion

3.1. Single step fabrication of the biomaterial-based microparticles

In this work, biomaterial-based microparticles were fabricated in a single step by a $CaCO_3$ template-directed supramolecular coordination chemistry technique. This innovative concept combines template synthesis and biomolecule assembly in one step, providing a robust and simple method for fabrication of highly homogeneous biomaterial-based microparticles. The spherical porous $CaCO_3$ formed from the co-precipitation reaction between $CaCl_2$ and Na_2CO_3 provided a sacrificial scaffold for preparing particles with well-defined size and morphology.[27,41] The entrapped biomolecules simultaneously interact with the Ca^{2+} in the reaction medium during template formation, in which the biomolecules undergo self-assembly driven by Ca^{2+} coordination chemistry, resulting in construction of supramolecular structure within the $CaCO_3$ template in a single step. The $CaCO_3$ templates were then removed by adjusting the pH to 5.0 with HCl, leaving behind pure biomaterial-based microparticles (Fig. 1).

The versatility of the developed technology for producing different biomaterial-based microparticles has been demonstrated here by using carbohydrate (alginate) and proteins (casein and fresh milk) as models. Fig. 2A–C show the optical images of the alginate, casein and milk microparticles, respectively. All three kinds of microparticles fabricated using this facile protocol are spherical in shape. Pure biomaterial-based microparticles with a concentration of 10^6–10^7 particles per mL can be obtained within 40 min. The measured average diameters of alginate, casein and milk microparticles were 2.37 μm (polydispersity = 0.23), 2.70 μm (polydispersity = 0.29)

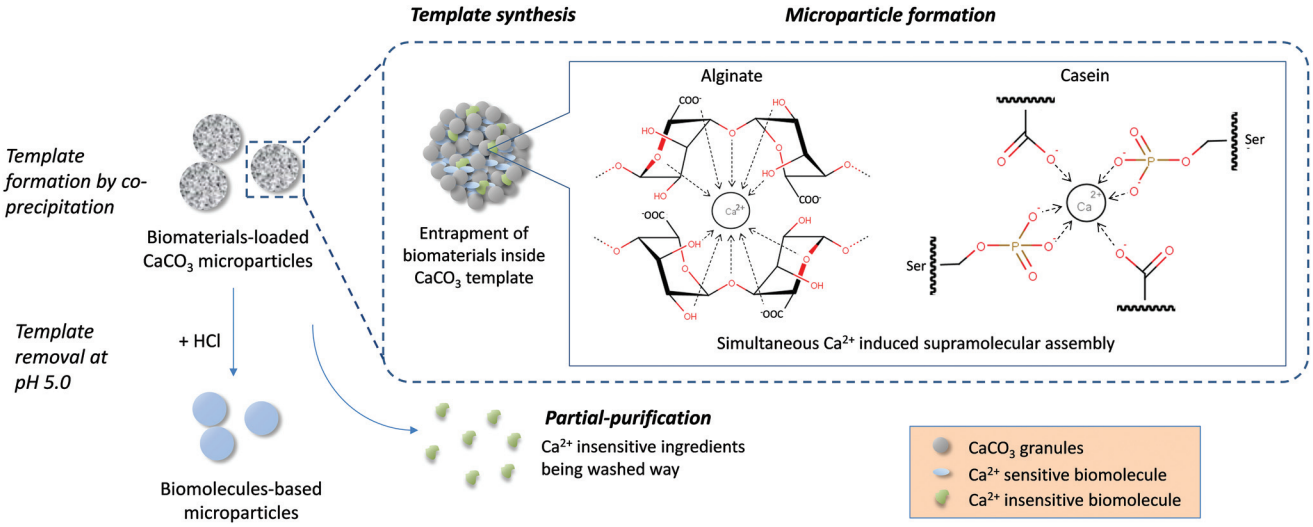

Fig. 1 Schematic diagram showing the single-step microparticle fabrication procedure combining template synthesis, biomolecule assembly and partial-purification for high efficiency fabrication of pure biomaterial-based microparticles. Ca^{2+} induced simultaneous assembly of alginate monomers according to the egg-box model.[30] For caseins, Ca^{2+} interacted with phosphoserine residues and carboxylate groups on the peptide chains of both β and α_s caseins.[38–40]

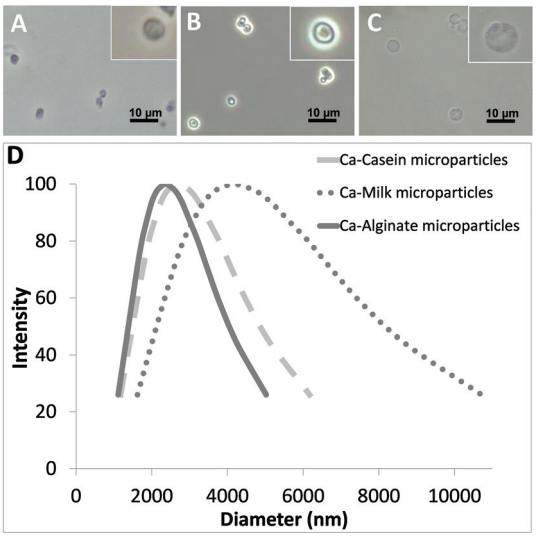

Fig. 2 Optical images of (A) alginate; (B) casein; and (C) milk microparticles. (D) Size distribution curves of the microparticles.

and 4.17 μm (polydispersity = 0.39), respectively (Fig. 2D). It is important to note that the average diameters of individual sets of alginate, casein and milk microparticles were different, although the concentration of the $CaCl_2$ and Na_2CO_3, and the reaction conditions (*e.g.* stirring speed, temperature, *etc.*) were kept constant for all three models. For instance, the alginate and casein microparticles showed narrower size distributions than milk microparticles. This could be explained by the $CaCO_3$ co-precipitation process, which governs the size of the resulting template. In the presence of different biomolecules (*i.e.* alginate, casein, and milk), formation of $CaCO_3$ will be slightly affected due to the viscosity of the matrix. An increase in viscosity will slow down the $CaCO_3$ co-precipitation process, providing a longer time for $CaCO_3$ growth and resulting in the formation of a $CaCO_3$ template with larger diameters. In contrast, a faster $CaCO_3$ co-precipitation process will lead to rapid depletion of Ca^{2+} and CO_3^{2-} in the mixture, limiting $CaCO_3$ growth, and thus resulting in smaller particle size.

The alginate and casein microparticles were produced using purified biomolecules with initial concentrations of 5 mg mL^{-1} alginate and 20 mg mL^{-1} casein, respectively. The relatively higher concentration in casein increased the viscosity of the reaction mixture, and therefore the average size of the casein microparticles is slightly larger than the alginate microparticles (1.14 times). For the case of milk microparticles, their size appeared to be significantly larger compared with both casein microparticles (1.54 times) and alginate microparticles (1.76 times). This can be explained by the much higher protein content (mainly casein) present in fresh milk (35 mg mL^{-1}), as well as in other ingredients such as fat and lactose, which augmented the matrix complexity.

3.2. Proof of Ca^{2+} coordination chemistry driven microparticle formation

To prove that Ca^{2+} coordination chemistry drives the formation of the biomaterial-based microparticles, the concentration of Ca^{2+} in the microparticles after template removal was determined using a commercial kit. The amounts of Ca^{2+} in alginate, casein, and milk microparticle suspensions were evaluated to be 99.76, 36.65, and 14.27 μM, respectively. For accurate comparison, the basal Ca^{2+} concentrations of alginate, casein and milk were measured and calculated to be 14.70, 15.75, and 24.58 μM, respectively (Table 1). It was found that Ca^{2+} content in alginate and casein microparticles is

Table 1 Summary of calcium ion concentration in (A) alginate microparticles, casein microparticles and milk microparticles, and (B) alginate solution, casein solution, and milk

		Alginate	Casein	Milk
(A)	Calcium in microparticle suspension (μM)	99.76	36.65	14.27
(B)	Basal calcium in corresponding solution (μM)	14.70	15.75	24.58
	No. of microparticles per mL	2.0×10^8	1.8×10^7	1.7×10^7
(A)/(B)		6.79	2.33	0.58
(A)–(B)	Additional calcium ions bound (μM)	85.06	20.90	−10.31
(C)	No. of additional calcium molecules per microparticle	2.6×10^8	6.9×10^8	—
(D)	No. of building block molecules per microparticle	1.2×10^7	8.3×10^7	—
(C) : (D)		22.1 : 1	8.3 : 1	—

M_w of alginate ~240 000; M_w of β-casein ~24 000.

6.79 times and 2.33 times higher than their corresponding basal calcium content, which is referred to as (A)/(B). It was shown that the basal calcium content for alginate and casein were very similar, while the calcium content in alginate microparticles was significantly higher than in the casein microparticles. This is likely due to the linear structure of the alginate molecules that allows binding of higher number of Ca^{2+} compared with the globular folded structure of casein molecules. After deducting the basal Ca^{2+} content from the controls, the net Ca^{2+} intake by the alginate and casein microparticle samples were calculated to be 85.06 and 20.90 μM, respectively. This significant increase could be explained by the involvement of Ca^{2+} in the formation of microparticles *via* coordination chemistry, where Ca^{2+} acted as metallic bridging molecules for crosslinking the biomolecules. There may also be some Ca^{2+} electrostatically interacting with the microparticle surface functional groups such as COO^-. However, this is trivial as the ratio of functional groups constituting the whole microsphere volume to those located at the surface is much higher. By further evaluating the number of microparticles in the samples and the amount of building blocks per microparticle, the molecular ratio between Ca^{2+} and building block molecules was deduced. The molecular ratio between Ca^{2+} and alginate was calculated to be ~22 : 1, while the molecular ratio between Ca^{2+} and casein was calculated to be ~8 : 1. Assuming that all additional Ca^{2+} contributed to the formation of metallic coordination bonds, there would be a maximum of 22 metallic coordination bonds between adjacent alginate molecules and 8 metallic coordination bonds between adjacent casein molecules involved in microparticle formation. The details of the Ca^{2+} induced crosslinking can be explained as follows. For the case of alginate, Ca^{2+} induced the crosslinking between two neighboring alginate chains by fitting into the G monomeric units as described by the 'egg-box' model.[30] The carboxylate and hydroxyl groups from each unit coordinated with the central Ca^{2+} forming a 3D network.[42] For casein, Ca^{2+} interacted with phosphoserine residues and carboxylate groups on both β and α_s caseins.[38–40] Oxygen moieties from these residues fit into the octahedral coordination sphere of Ca^{2+}, forming inter and intra-protein bridges.

In contrast, Ca^{2+} content in milk microparticles was shown to be around 40% less than that in fresh milk. This phenomenon can be explained by the fact that fresh milk is itself a calcium rich source. Microscopically, native caseins in milk self-assemble into micelles in the presence of calcium phosphate. When they are in contact with a high concentration of free Ca^{2+}, the micelle structure breaks down, with the Ca^{2+} sensitive β-caseins assembled together but the remaining constituents, including other Ca^{2+} insensitive peptides (*e.g.* κ-casein) and calcium phosphates, washed away.[43–45] Therefore, although it is certain that the β-caseins in fresh milk has formed microparticles *via* Ca^{2+} induced supramolecular assembly, the lower overall Ca^{2+} content in the milk microparticles could be explained by the disruption of the micelle structure and the loss of native calcium phosphates during the microparticle fabrication process.

3.3. Surface morphologies and zeta potential of the biomaterial-based microparticles

To study the morphology of microparticles in greater detail, SEM images of the microparticles before and after template removal were obtained. The structure of the $CaCO_3$ template consists of microgranules with a uniform size of about 10–30 nm.[16] During the coprecipitation process between $CaCl_2$ and Na_2CO_3, the granules were formed by nucleation, followed by assembly of multiple granules into a spherical structure with interconnected vacant space/pores (Fig. S1†). Biomolecules present in the reaction mixture were simultaneously entrapped within the pores of the $CaCO_3$ template and subsequently crosslinked *via* Ca^{2+} coordination chemistry, forming the microparticles.

The use of $CaCO_3$ templating in microparticle fabrication has several advantages. First of all, the size of final microparticles can be controlled by adjusting the dimensions of $CaCO_3$ templates, since microparticles are constructed inside, and thus limited in size by, the templates. This can be easily accomplished by adjusting experimental parameters such as stirring time, stirring speed, *etc*.[27] Secondly, in this protocol, the biomolecules are crosslinked almost instantaneously. In contrast to existing protocols involving extra incubation steps lasting from hours to days,[25,26] our less time intensive single-step approach offers greater practicability for scaling up. Last but not least, the template can be thoroughly removed after the microparticles were formed. As $CaCO_3$ is soluble in mild

acidic pH environments, the template can be removed simply by titration with a mild acid. It was observed that the template can be removed at pH 5. With subsequent washing by d.d. H_2O, pure biomaterial-based microparticles can be yielded.

Before template removal, the surface of alginate, casein and milk microparticles were observed to be rough (Fig. 3Ai, Bi and Ci). The granular structures of $CaCO_3$ templates were clearly observed under high magnification images (inserts of Fig. 3Ai and Bi). For the case of milk particles, the $CaCO_3$ template was fully covered by the crosslinked casein (Fig. 3Ci), which is likely due to the high protein content in milk. After $CaCO_3$ template removal, the alginate microparticles resembled flattened circular discs, mainly due to drying and high vacuum conditions during SEM imaging (Fig. 3Aii), whereas the casein and milk microparticles remained as spheres (Fig. 3Bii and Cii). The difference in the morphologies among alginate, casein and milk microparticles in the dried SEM microparticle samples can be further explained by the difference in chemical structures between alginate and casein. Alginate is a linear hydrophilic biopolymer that can form a relatively low-density Ca^{2+}-alginate hydrogel network with high water holding capacity.[46] Since our preparation protocol took place in an aqueous environment, the alginate particles formed were intrinsically swollen due to high water content. Therefore, the dried alginate microparticle after water removal appeared flattened and collapsed.

In contrast, casein is a globular protein. After Ca^{2+} coordination crosslinking, the adjacent casein molecules were connected into a relatively higher-density network with lower water holding capacity. Therefore, the casein microparticles remained as 3D spheres in the SEM images. A similar explanation is applied for the milk microparticles, where the major protein content is also casein. In addition, the magnified SEM images of both the casein and milk microparticle surfaces (insert of Fig. 3Bii and Cii) revealed rigid crests and obvious shadows, while the surface of alginate particles appeared to be smooth and flattened. The sizes of different microparticle samples with the $CaCO_3$ template were deducted from the SEM images. It was found that the diameters for both the casein and milk microparticles were ~10% smaller compared with the template size (*i.e.* before $CaCO_3$ template removal), while the size of the alginate microparticles was ~12% larger compared with the template size. This finding is consistent with our previous discussion that casein molecules with globular structure were interconnected into a relatively high-density network causing a slight decrease in microparticle diameter due to shrinking, while alginate molecules with a linear structure were interconnected into a relatively low-density hydrogel network causing a slight increase in microparticle diameter due to swelling.

To understand the colloidal stability of the microparticles under physiological pH conditions, we further examined the surface charge of the microparticles by zeta potential analysis. As shown in Fig. 4A, the measured zeta potential (at pH 7.0) of alginate, casein, and milk microparticles were −25.49 mV (± 2.02 mV), −21.51 mV (± 2.02 mV), and −22.02 mV (± 6.27 mV), respectively. The negative zeta potential values from all three samples can be explained by the functional groups present on the particle surface. For alginate microparticles, the pK_a value of alginate is around pH 3.5. Therefore at pH 7.0, the carboxylic groups of the alginate are readily deprotonated and become negatively charged. Although some of the carboxylic groups in the alginate microparticles are crosslinked by the positively charged Ca^{2+} according to the egg-box model, an abundance of free carboxylic acid groups within the alginate polymer backbone contributes to the negative zeta potential.

In the cases of casein and milk microparticles, their core component is β-casein, which has an isoelectric point of 4.5. Therefore at physiological pH, β-casein carries a net negative charge. From a molecular point of view, β-casein is rich in phosphoserine residues and carboxylate groups, which perhaps further contributed to the negative zeta potential at pH 7.0. In general, all three kinds of microparticles have zeta

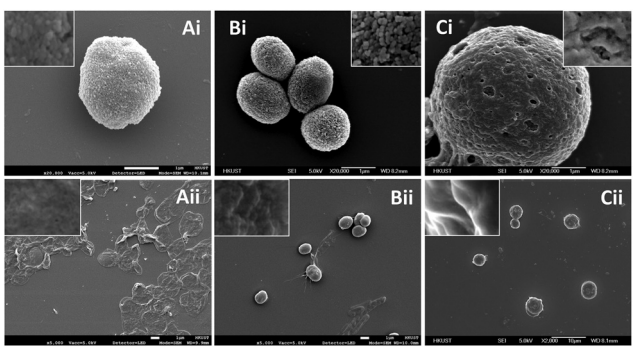

Fig. 3 Scanning electron micrographs of: (A) alginate microparticles, (B) casein microparticles and (C) milk microparticles (i) within the $CaCO_3$ template and (ii) after template removal, respectively. Insets show the high magnification images of the microparticle surfaces.

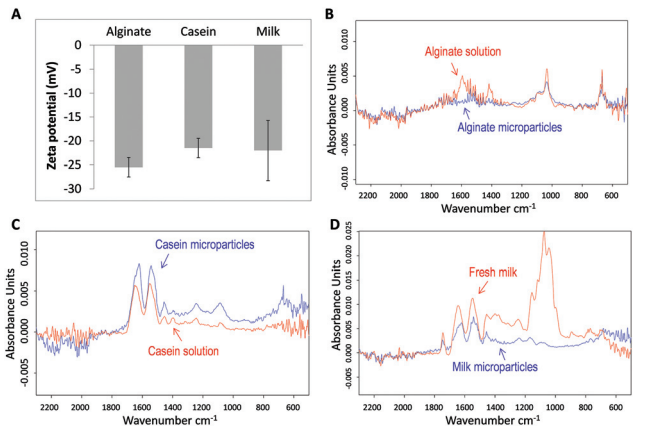

Fig. 4 (A) Zeta potentials of alginate; casein; and milk microparticles, respectively. FTIR spectrum of (B) alginate solution and microparticles; (C) casein solution and microparticles; and (D) fresh milk and microparticles.

potentials with magnitude larger than −20 mV, suggesting significant surface charge and good colloidal stability.[47]

3.4. Chemical and secondary structure analysis

For investigation of the chemical structure of biomolecules after formation into microparticles, Fourier transform infrared (FTIR) spectra were obtained and analyzed. A set of control spectra including alginate solution, casein solution, and milk were also obtained for comparison. For the spectrum of alginate samples (Fig. 4B), a conserved region from 800 to 1200 cm^{-1} is found in both the alginate solution and the corresponding microparticles. A characteristic main band near 1029 cm^{-1} corresponds to the conserved carbohydrate band originating from the C–O, C–C, and C–O–H bonds in both the alginate solution and microparticles.[48,49] At 1550–1610 cm^{-1} an obvious band is observed for the alginate solution but not in the microparticles. The flattening of the signal in this region may be due to the interaction between Ca^{2+} and COO^{-} groups of alginate monomers. After forming the coordination complex, vibration of the carboxylate group is restricted, rendering a diminished signal in the spectrum.[50] Some of the COO^{-} groups on the particle surface may also have electrostatic interactions with Ca^{2+}. Similarly for the region from 1395 to 1440 cm^{-1}, the absence of the band in alginate microparticles reflects reduced COO^{-} stretching and C–O–H bending. Both groups are involved in the coordination binding with Ca^{2+}.[51,52] These results not only revealed the conservation of major structures but also gave evidence of Ca^{2+} induced supramolecular assembly within alginate microparticles.

For casein samples, the spectrum of casein microparticles revealed a high degree of resemblance to that of casein solution (Fig. 4C). The main bands at 1640 cm^{-1} and 1550 cm^{-1} correspond to amide I and amide II, which are interpreted as the alpha-helix and the beta-sheet.[53] The area ratios under the bands of the casein solution and microparticles are similar. A slight shift of bands at 1640 cm^{-1} towards 1620 cm^{-1} was observed for casein microparticles. This might show that some of the alpha-helixes were slightly reconfigured resulting from the Ca^{2+} coordination chemistry after microparticle formation.[54] Except this band, most other secondary structures of casein in microparticles resembled native molecules. For the milk samples, two main bands in the region of 1500–1700 cm^{-1} are conserved, indicating that significant amounts of alpha-helixes and beta-sheets are preserved in milk microparticles (Fig. 4D). Similar to the case of casein microparticles, the band at 1640 cm^{-1} has also been shifted to 1620 cm^{-1}. This observation can be attributed to the high presence of casein in milk, making up to 80% of its protein content. In the regions of 1200–1450 cm^{-1} and 800–1200 cm^{-1}, the absorbance curve appeared to be flattened in milk microparticles. The weaker absorption signal in these two regions could be interpreted to be caused by removal of the non-crosslinked proteins and carbohydrates during the microparticle fabrication process. It is hypothesized that during the formation of milk microparticles, the high concentration of free Ca^{2+} ions breaks down the native casein micelles and binds with Ca^{2+} sensitive proteins (*e.g.* α_s and β-casein) forming a supramolecular structure. Meanwhile, the Ca^{2+} insensitive components were removed from the $CaCO_3$ template during the washing procedures, which accounts for the reduced absorbance in the region of 1200–1450 cm^{-1}. The strong band in the spectrum of fresh milk at the region of 800–1200 cm^{-1} is possibly contributed by the high lactose concentration in milk, about 5% of the total content.[55] The absence of this band in the milk microparticle spectrum suggests that lactose was absent in the milk microparticles. This proves that the concept of partial purification during microparticle fabrication is successful. On the other hand, the conserved regions between the spectra of microparticles and their raw materials prove that the chemical and secondary structures of the biomaterials are mostly conserved under crosslinking by the relatively mild Ca^{2+} coordination chemistry conditions.

3.5. Selective crosslinking and purified biomaterial-based microparticles

Another unique advantage of the template-directed crosslinking method is fabrication of purified biomaterial-based microparticles from a relatively complex biological mixture. In this context, we demonstrate the idea by studying the formation of casein microparticles from complex casein in fresh milk and from purified casein. Our hypothesis is that only the Ca^{2+} sensitive proteins in the fresh milk will be crosslinked within the $CaCO_3$ template, followed by a template-assisted partial-purification process in which other non-crosslinked components will be washed away from the complex mixture. Finally, we could obtain relatively pure microparticles composed of only the selectively crosslinked proteins. In order to prove this hypothesis, the protein contents in casein and milk microparticles were assessed by sodium dodecyl sulfate polyacrylamide gel electrophoresis (SDS-PAGE), with the native casein solution and fresh milk as controls (Fig. 5). The protein band pattern of casein microparticles (lane B) is identical to

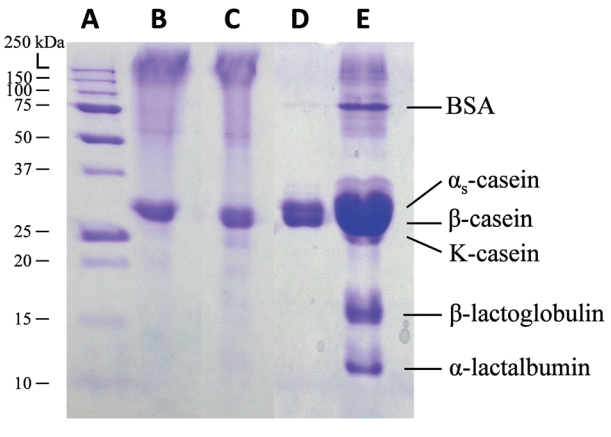

Fig. 5 SDS-PAGE of (A) molecular weight ladder, (B) casein microparticles, (C) casein solution, (D) milk microparticles, and (E) diluted fresh milk.

native casein solution (lane C). This shows that the casein microparticles are composed of pure casein as all the protein components are conserved. In contrast, milk microparticles showed only 2 protein bands (lane D), with missing bands—when compared to fresh milk (lane E)—indicating the absence of a number of other proteins. According to the protein fractions identified in the milk samples, the proteins present in the milk microparticles are α_s and β-casein.[56] These two proteins are known to be Ca^{2+} sensitive, and had thus assembled into a stable structure in the presence of Ca^{2+} ions. Other proteins including BSA, κ-casein, β-lactoglobulin, and α-lactalbumin originally present in the milk are absent in the milk microparticles. These proteins do not react with Ca^{2+} ions, and were thus washed away during microparticle formation. This result further supports the formation of microparticles as selectively driven by Ca^{2+} coordination chemistry (*i.e.* not by non-specific protein aggregation). The results of protein content analysis by SDS-PAGE—absence of other non-crosslinked ingredients in the milk—also explains the significant reduction of the absorbance band from 1200 to 1450 cm^{-1} in the FTIR spectrum of milk microparticles (Fig. 4D). Inherent purification of raw materials during the fabrication process is both cost and time-effective, obviating the need for extra material pre-treatment steps prior to the fabrication process.

4. Conclusions

Biomaterial-based microparticles were fabricated by a novel single-step approach *via* template-directed supramolecular coordination chemistry. We have demonstrated the fabrication of carbohydrate (alginate) microparticles, as well as protein (casein) microparticles from both casein solution and complex non-purified biomaterial (fresh milk). All three types of microparticles showed no significant aggregation or degradation over a storage period of more than 6 months in 4 °C, which is important for drug storage and other pharmaceutical applications. Quantitative analysis has proven that formation of microparticle is selectively driven by supramolecular assembly *via* Ca^{2+} coordination chemistry, and not *via* non-specific protein aggregation. The specific Ca^{2+} coordination chemistry simultaneously excludes non-specific materials from the template and provides an additional partial-purification function to produce relatively pure casein microparticles from complex fresh milk, as proven by SDS-PAGE analysis. Moreover, owing to mild fabrication conditions, most of the chemical and secondary structures of the biomolecules in microparticles were conserved, as proven by FTIR spectroscopy. This high efficiency manufacturing processes provides a robust and green chemistry method to fabricate biomaterial-based microparticles, with the cardinal advantage being elimination of upstream purification processes and use of synthetic crosslink reagents, thus addressing recent concerns of energy and environmental conservation in manufacturing processes. By extension, through use of the $ZnCO_3$ template as opposed to $CaCO_3$, the presented approach may potentially apply to the fabrication of microparticles driven by Zn^{2+} mediated protein and peptide macromolecular complex formation.[57,58]

Notes and references

1 K. Saralidze, L. H. Koole and M. L. W. Knetsch, *Materials*, 2010, **3**, 3537–3564.
2 Y. H. Won, H. S. Jang, D. W. Chung and L. A. Stanciu, *J. Mater. Chem.*, 2010, **20**, 7728.
3 B. M. A. N. Estevinho, F. A. N. Rocha, L. M. D. S. Santos and M. A. C. Alves, *J. Microencapsulation*, 2013, **30**, 571–579.
4 A. Jefferson, R. S. Wijesurendra, M. A. McAteer, J. E. Digby, G. Douglas, T. Bannister, F. Perez-Balderas, Z. Bagi, A. C. Lindsay and R. P. Choudhury, *Atherosclerosis*, 2011, **219**, 579–587.
5 L. Chen, G. E. Remondetto and M. Subirade, *Trends Food Sci. Technol.*, 2006, **17**, 272–283.
6 B. H. Jun, H. Kang, Y. S. Lee and D. H. Jeong, *Molecules*, 2012, **17**, 2474–2490.
7 M. B. Oliveira and J. F. Mano, *Biotechnol. Prog.*, 2011, **27**, 897–912.
8 S. S. Kuang, J. C. Oliveira and A. M. Crean, *Crit. Rev. Food Sci. Nutr.*, 2010, **50**, 951–968.
9 C. Engman, Y. Wen, W. S. Meng, R. Bottino, M. Trucco and N. Giannoukakis, *Clin. Immunol.*, 2015, **160**, 103–123.
10 Y. Wen and J. H. Collier, *Curr. Opin. Immunol.*, 2015, **35**, 73–79.
11 C. Chung, B. Degner and D. J. McClements, *Food Res. Int.*, 2014, **64**, 664–676.
12 C. Kusonwiriyawong, W. Pichayakorn, V. Lipipun and G. C. Ritthidej, *J. Microencapsulation*, 2009, **26**, 111–121.
13 J. R. Howse, R. A. L. Jones, G. Battaglia, R. E. Ducker, G. J. Leggett and A. J. Ryan, *Nat. Mater.*, 2009, **8**, 507–511.
14 W. Lin, A. G. Coombes, M. C. Davies, S. S. Davis and L. Illum, *J. Drug Targeting*, 1993, **1**, 237–243.
15 N. G. Balabushevich, V. A. Izumrudov and N. I. Larionova, *Polym. Sci., Ser. A*, 2012, **54**, 540–551.
16 E. M. Pouget, P. H. H. Bomans, J. A. C. M. Goos, P. M. Frederik, G. de With and N. A. J. M. Sommerdijk, *Science*, 2009, **323**, 1455–1458.
17 D. Preisig, D. Haid, F. J. O. Varum, R. Bravo, R. Alles, J. Huwyler and M. Puchkov, *Eur. J. Pharm. Biopharm.*, 2014, **87**, 548–558.
18 A. M. Yashchenok, D. Borisova, B. V. Parakhonskiy, A. Masic, B. Pinchasik, H. Möhwald and A. G. Skirtach, *Ann. Phys.*, 2012, **524**, 723–732.
19 Z. She, C. Wang, J. Li, G. B. Sukhorukov and M. N. Antipina, *Biomacromolecules*, 2012, **13**, 2174–2180.
20 K. Sato, M. Seno and J.-I. Anzai, *Polymers*, 2014, **6**, 2157–2165.
21 X. Yan, J. Li and H. Möhwald, *Adv. Mater.*, 2012, **24**, 2663–2667.
22 S. Satya Prakash, *Int. J. Nanomed.*, 2010, 525.
23 S. Vino, K. R. Lokesh, S. Vijayaragavan, G. Jayaraman and A. R. Ghosh, *Int. J. Pharm. Sci. Res.*, 2011, **2**, 383–390.

24 W. J. Tong, C. Y. Gao and H. Möhwald, *Colloid Polym. Sci.*, 2008, **286**, 1103–1109.
25 Z. Li, Y. Zhang, Y. Su, P. Ouyang, J. Ge and Z. Liu, *Chem. Commun.*, 2014, **50**, 12465–12468.
26 J. Ge, J. Lei and R. N. Zare, *Nat. Nanotechnol.*, 2012, **7**, 428–432.
27 W. C. Mak, R. Georgieva and R. Renneberg, *Adv. Funct. Mater.*, 2010, **20**, 4139–4144.
28 S. M. Sood and C. W. Slatter, *J. Dairy Sci.*, 2002, **85**, 1353–1356.
29 J. Sun and H. Tan, *Materials*, 2013, **6**, 1285–1309.
30 P. Sikorski, F. Mo, G. Skjåk-Bræk and B. T. Stokke, *Biomacromolecules*, 2007, **8**, 2098–2103.
31 Z. Xu, *Sci. Rep.*, 2013, **3**, 2914.
32 N. Holten-Andersen, M. J. Harrington, H. Birkedal, B. P. Lee, P. B. Messersmith, K. Y. C. Lee and J. H. Waite, *Proc. Natl. Acad. Sci. U. S. A.*, 2011, **108**, 2651–2655.
33 R. Furukawa, A. Maselli, S. A. M. Thomson, R. W. L. Lim, J. V. Stokes and M. Fechheimer, *J. Cell Sci.*, 2003, **116**, 187–196.
34 P. K. Hepler and L. J. Winship, *J. Integr. Plant Biol.*, 2010, **52**, 147–160.
35 B. D. Smith, P. L. La Celle, G. E. Siefring, L. Lowe-Krentz and L. Lorand, *J. Membr. Biol.*, 1981, **61**, 75–80.
36 D. Pyo, *Bull. Korean Chem. Soc.*, 2009, **30**, 1215–1217.
37 M. Mishra and B. Mishra, *Yakugaku Zasshi*, 2011, **131**, 1813–1825.
38 D. M. Byler and H. M. Farrell Jr., *J. Dairy Sci.*, 1989, **72**, 1719–1723.
39 K. J. Cross, N. L. Huq, J. E. Palamara, J. W. Perich and E. C. Reynolds, *J. Biol. Chem.*, 2005, **280**, 15362–15369.
40 S. Marchesseau, J. C. Mani, P. Martineau, F. Roquet, J. L. Cuq and M. Pugnière, *J. Dairy Sci.*, 2002, **85**, 2711–2721.
41 N. Sudareva, H. Popova, N. Saprykina and S. Bronnikov, *J. Microencapsulation*, 2014, **31**, 333–343.
42 D. Kuhbeck, J. Mayr, M. Haring, M. Hofmann, F. Quignard and D. Diaz Diaz, *New J. Chem.*, 2015, **39**, 2306–2315.
43 C. Guo, B. E. Campbell, K. Chen, A. M. Lenhoff and O. D. Velev, *Colloids Surf., B*, 2003, **29**, 297–307.
44 P. Müller-Buschbaum, R. Gebhardt, S. V. Roth, E. Metwalli and W. Doster, *Biophys. J.*, 2015, **93**, 960–968.
45 D. G. Dalgleish, *Soft Matter*, 2011, **7**, 2265.
46 C. K. Kuo and P. X. Ma, *J. Biomed. Mater. Res., Part A*, 2008, **84**, 899–907.
47 S. Honary and F. Zahir, *Trop. J. Pharm. Res.*, 2013, **12**, 255–264.
48 C. G. van Hoogmoed, H. J. Busscher and P. de Vos, *J. Biomed. Mater. Res., Part A*, 2003, **67**, 172–178.
49 P. Li, Y. N. Dai, J. P. Zhang, A. Q. Wang and Q. Wei, *Int. J. Biomed. Sci.*, 2008, **4**, 221–228.
50 J. Coates, in *Encyclopedia of Analytical Chemistry*, 2000, pp. 10815–10837.
51 G. A. Paredes Jurez, M. Spasojevic, M. M. Faas and P. de Vos, *Front. Bioeng. Biotechnol.*, 2014, **2**, 1–15.
52 K. Kashima and M. Imai, *InTech*, 2012, 3–36.
53 C. Van der Ven, S. Muresan, H. Gruppen, D. B. A. De Bont, K. B. Merck and A. G. J. Voragen, *J. Agric. Food Chem.*, 2002, **50**, 6943–6950.
54 Y. Wen, S. L. Roudebush, G. a. Buckholtz, T. R. Goehring, N. Giannoukakis, E. S. Gawalt and W. S. Meng, *Biomaterials*, 2014, **35**, 5196–5205.
55 M. Solís-Oba, O. Teniza-García, M. Rojas-López, R. Delgado-Macuil, J. Díaz-Reyes and R. Ruiz, *J. Mex. Chem. Soc.*, 2011, **55**, 190–193.
56 F. F. Costa, M. A. Vasconcelos Paiva Brito, M. A. Moreira Furtado, M. F. Martins, M. A. de Oliveira, P. de Castro Barra, L. Amigo Garrido and A. de Oliveira dos Santos, *Anal. Methods*, 2014, **6**, 1666–1673.
57 M. Laitaoja, J. Valjakka and J. Jänis, *Inorg. Chem.*, 2013, **52**, 10983–10991.
58 N. Pace and E. Weerapana, *Biomolecules*, 2014, **4**, 419–434.